

# SIMULATION OF A TENNIS PLAYER'S SWING-ARM MOTION

Hyounkyun Oh, Savannah State University; Onaje Lewis, Georgia Institute of Technology; Asad Yousuf, Savannah State University; Sujin Kim, Savannah State University

## Abstract

Human-factors modeling and the simulation of the human movement have been critical bases for finding the optimized motion in a variety of areas. This study investigated both aspects: the mechanical modeling of the human arm structure and the computational simulation and analysis of a tennis player's full-swing motion, while the player receives a ball. For this objective, the arm structure was regarded as a serial 6 degrees of freedom (DOF) mechanical manipulator with three rigid links. Each joint-angle data point was obtained in a discrete manner through the observation of a related video file. The data were then applied to the Denavit-Hartenberg (DH) Convention to lead the position vectors of the shoulder, elbow, wrist, and the center point of the racket. The smooth position functions along the DH parameter ( $q_1$  through  $q_6$ ) were achieved through the cubic spline interpolation theory. The 3-dimensional graphical simulations were produced based on these smooth functions in MATLAB. Additionally, in order to measure the tennis player's quality of performance, the constraint functions of stress and potential energy were evaluated. The results of the analysis were expected to provide valuable information on a tennis player's full-swing motion and also serve as a guide for making optimal movements.

## Introduction

Human-factors modeling and the simulation of the human movement have been widely used as critical tools for implementing optimized human motion in a variety of areas including the factory floors: management constantly seeks better ways of organizing work space [1]; building-construction areas are ergonomically designed with barrier-free equipment or safe structure for physically disabled persons [2]-[7]; the improvement of the efficiency of troop movement on military fields [8]-[10], and so on. In particular, one of the most wide-open areas, where the analysis of the human body's movement is used, may be in the field of sports [11]-[13]. The analysis of the technical deficiencies of an athlete can assist the coach or teacher in identifying the areas where the athlete needs to improve his/her performance. In addition, this analysis can be applied for reforming the athlete's habitual motion, which may potentially cause repetitive fatigue or sudden injury. This study also analyzed the athlete's performance.

In tennis, athletes seek to perfect their swing so that the ball is placed on the desired point as accurately and as fast as possible. In other words, people have always wondered what the perfect forehand swing is in tennis. However, no one has come up with an exact explanation of what it is. This is mainly because human subjects are extremely complex and have intrinsic limitations. As humans are unquestionably the random variable, subject to fatigue, and have limitations of strength and coordination, they must be treated with a considerable measure of safety and ethics. Theoretically, the subject of the perfect swing motion may be summarized as an individual's optimization problem depending on the various cost functions such as personal discomfort, fatigue, effort, potential energy, dexterity, etc. Nevertheless, people have tried to mimic the world's top players' motions throughout the decades for many reasons; perhaps out of curiosity of top players' abilities and long experiences, or perhaps to investigate the best way to improve their athletic techniques or formulate techniques that would reduce stress on their arms.

The main objectives of this study were the implementation of a computational simulation of the world's top tennis player's forehand stroke, and the provision of biomechanical information by analyzing the simulation. The authors address these objectives in the following order:

- A general modeling method for a mechanical rigid body
- Collection of data through the observation of a video file
- Conversion of discrete data into smooth functions
- Computational simulation of the motion based on the smooth data in MATLAB
- Analysis of the simulation and optimization factors

## Method of Kinetic Modeling

Biomechanical investigations often involve a simplified mechanical model of a human body. Mass-spring-damper models are often used to model human movements in which impacts occur. Musculoskeletal models are mostly used for describing individual muscles [14]. For kinetic analyses, one of the most commonly used models is the rigid-body model. Rigid-body models represent the human system in whole or part as a set of rigid segments controlled by joint move-

ments. In other words, the human body is considered as a system of serial rigid manipulators, which are connected at easily-identifiable joints. Theories of anatomical and experimental mechanisms characterize joints of these manipulators so that a position vector can describe the location of the specific point in terms of all joint displacements. For example, Dapena [15] developed a 15-link segment model in his optimization of a high jump; Yeadon [16] used a rigid 11-segmental model with 17 degrees of freedom to describe the aerial movements of the human body. Figure 1 illustrates how the authors in this study segmented the arm structure [13], [17], [18].

In this study, the authors considered a mechanical system of three articulated rigid links that were composed of the upper arm from shoulder to elbow, the lower arm from elbow to wrist, and the hand-to-racket link from wrist to the center of the racket. It was assumed that body segments are rigid-links, and joints are frictionless and hinged. Each link was connected with two revolute joints, as shown in Figure 1. Information from anthropometry in occupational biomechanics, which deals with the measure of size, shape, mass, and inertial properties of the human body segments, was also considered.

The mechanism developed by the authors, then, was considered to have 6 degrees of freedom (DOF). Of course, more detailed modeling may be possible by adding the third revolute joint on the shoulder or two prismatic joints between the neck point and shoulder. Even though such complex models are more accurate at describing human behavior, the model introduced here was adequate for defining the arm swing motion.

The construction of an operating procedure for the calculation of direct kinematics is naturally derived from the typical open-kinematics chain of the manipulator structure. One of the preferable methods comes from the Denavit-Hartenberg (DH) convention, which is based on the fact that each joint connects two consecutive links. This convention

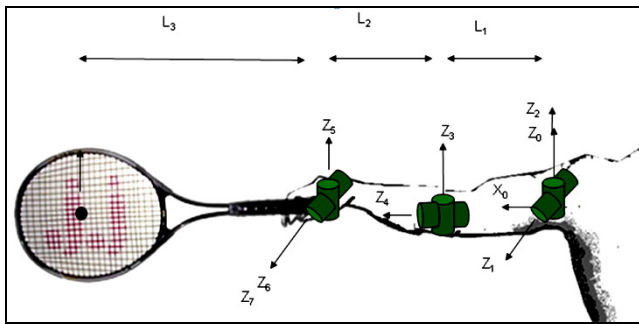


Figure 1. Modeling of segments & joints of the player's arm

considers first the description of kinematics relation between consecutive links and secondly the process to obtain the overall description of manipulator kinematics in a recursive fashion. Position vectors are determined in terms of all joint displacements [17], [18], and such a relation between adjacent links is expressed effectively from the DH method [19]. The DH method is based on the  $4 \times 4$  transformation matrix from the link  $i-1$  to the link  $i$ , which is defined by

$${}^{i-1}\mathbf{T}_i = \begin{bmatrix} \cos q_i & -\cos \alpha_i \sin q_i & \sin \alpha_i \sin q_i & a_i \cos q_i \\ \sin q_i & \cos \alpha_i \cos q_i & -\sin \alpha_i \cos q_i & a_i \sin q_i \\ 0 & \sin \alpha_i & \cos \alpha_i & d_i \\ 0 & 0 & 0 & 1 \end{bmatrix} \quad (1)$$

where  $q_i$  is the joint angle between the axes  $X_{i-1}$  and  $X_i$ ,  $d_i$  is the distance between these axes along the axis  $Z_i$ ,  $a_i$  is the offset distance from the intersection of  $Z_{i-1}$  with the axis  $X_i$ , and  $\alpha_i$  is the offset angle between  $Z_{i-1}$  and  $Z_i$  along the axis  $X_i$ . Then, the homogeneous matrix

$${}^0\mathbf{T}_n = {}^0\mathbf{T}_1 {}^1\mathbf{T}_2 \dots {}^{n-1}\mathbf{T}_n = \begin{bmatrix} {}^0\mathbf{R}_n(\mathbf{q}) & \mathbf{x}(\mathbf{q}) \\ 0 & 1 \end{bmatrix} \quad (2)$$

specifies the location of the  $i^{\text{th}}$  coordinate frame with respect to the base coordinate system. Here, the matrix  ${}^0\mathbf{R}_n(\mathbf{q})$  represents the rotation matrix and  $\mathbf{x}(\mathbf{q})$  represents the position vector. Thus, the position  $\mathbf{x}(\mathbf{q}^*)$  of the aimed end effector can be found by the rule

$$\begin{bmatrix} \mathbf{x}(\mathbf{q}^*) \\ 1 \end{bmatrix} = {}^0\mathbf{T}_n(q_1, \dots, q_n) \begin{bmatrix} \mathbf{x}_0 \\ 1 \end{bmatrix} \quad (3)$$

where  $\mathbf{x}_0$  is the starting point of the base coordinate system.

In order to obtain the DH parameters, Figure 2 illustrates the transformed directions of each reference frame and Table 1 shows the DH table matching with the diagram of frames.

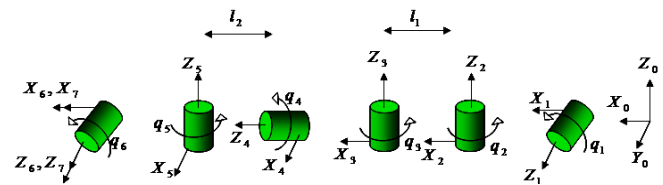


Figure 2. Segmental diagram of the arm for the DH methods

**Table 1. DH parameters for the arm structure**

|           | $q_i$       | $d_i$ | $\alpha_i$ | $a_i$ |
|-----------|-------------|-------|------------|-------|
| ${}^0T_1$ | 0           | 0     | -90        | 0     |
| ${}^1T_2$ | $q_1$       | 0     | 90         | 0     |
| ${}^2T_3$ | $q_2$       | 0     | 0          | $l_1$ |
| ${}^3T_4$ | $90 + q_3$  | 0     | 90         | 0     |
| ${}^4T_5$ | $q_4$       | $l_2$ | -90        | 0     |
| ${}^5T_6$ | $-90 + q_5$ | 0     | -90        | 0     |
| ${}^6T_7$ | $q_6$       | 0     | 0          | $l_3$ |

Based on this information, each position vector of the shoulder (considered the starting point) elbow, wrist and the center of the racket is given as

$$\text{Shoulder position} = [0,0,0]^T \quad (4a)$$

$$\text{Elbow position} = [l_1s_2, -l_1c_1c_2, -l_1s_1c_2]^T \quad (4b)$$

$$\text{Wrist position} = \begin{pmatrix} l_2s_2c_3 + l_2c_2s_3 + l_1s_2 \\ -c_1(l_2c_2c_3 - l_2s_2s_3 + l_1c_2) \\ -s_1(l_2c_2c_3 - l_2s_2s_3 + l_1c_2) \end{pmatrix} \quad (4c)$$

$$\text{Racket center position} = \begin{pmatrix} -l_3c_6c_4s_5s_2s_6 + \dots + l_2c_2s_3 + l_1s_2 \\ l_3c_6s_5c_4c_1c_2s_3 + \dots + l_2c_1s_2s_3 - l_1c_1c_2 \\ l_3c_6s_5c_4s_1c_2s_3 + \dots + l_2s_1s_2s_3 - l_1s_1c_2 \end{pmatrix} \quad (4d)$$

Here,  $c_i$  and  $s_i$  represent  $\cos(q_i)$  and  $\sin(q_i)$ , respectively. This analysis applied the used joint variables to the optimization problems.

## Data Correction

The video used in this study for simulation was captured from a shot, while the world's number one player, Federer, hit at Wimbledon. The file was initially slowed down by 1000 frames per second, in order to calculate the actual speed of the swing. Time and speed were measured using Windows Movie Maker. The video's frame rate was 25 frames per second and lasted 14 seconds. Thus, the actual swing time was calculated at  $x = 0.35$  seconds from

$$\frac{1000 \text{ frames/sec}}{25 \text{ frames/sec}} = \frac{14 \text{ seconds}}{x \text{ seconds}} \quad (5)$$

Each angle along the swing was broken up into 17 time-intervals with increments of 0.0206 seconds. The point of impact was at roughly 1.5 seconds but was not measured in increments of 0.0206 seconds. Figure 3 shows one cut of the video file and Table 2 shows the observed joint angles during the player's full motion.



**Figure 3. Screen capture from the video file**

**Table 2. Collected angle data from the video file (Unit: degree)**

|            | $q_1$ | $q_2$ | $q_3$ | $q_4$ | $q_5$ | $q_6$ |
|------------|-------|-------|-------|-------|-------|-------|
| 0.0000 sec | 40    | -35   | 20    | -45   | -40   | -45   |
| 0.0206 sec | 42    | -30   | 15    | -43   | -45   | -38   |
| 0.0412 sec | 45    | -25   | 10    | -38   | -55   | -35   |
| 0.0618 sec | 50    | -15   | 5     | -23   | -60   | -23   |
| 0.0824 sec | 60    | 0     | 3     | -15   | -70   | -15   |
| 0.1029 sec | 50    | 10    | 0     | -10   | -90   | -3    |
| 0.1235 sec | 42    | 30    | 0     | -8    | -100  | 0     |
| 0.1441 sec | 35    | 60    | 0     | -3    | -120  | 0     |
| 0.1647 sec | 25    | 70    | 5     | 0     | -95   | 10    |
| 0.1853 sec | 23    | 80    | 15    | 10    | -60   | 25    |
| 0.2059 sec | 22    | 90    | 22    | 20    | -10   | 30    |
| 0.2265 sec | 21    | 105   | 32    | 30    | 0     | 20    |
| 0.2471 sec | 20    | 120   | 50    | 45    | 0     | 20    |
| 0.2676 sec | 18    | 145   | 90    | 80    | 0     | 20    |
| 0.2882 sec | 15    | 160   | 92    | 85    | 0     | 20    |
| 0.3088 sec | 13    | 165   | 94    | 95    | 5     | 20    |
| 0.3294 sec | 7     | 180   | 97    | 100   | 10    | 20    |
| 0.3500 sec | 6     | 180   | 100   | 105   | 15    | 20    |

It is important to note that the image from the video file was seen from one viewing point. As a result, the exact measurement of the joint angles was difficult or almost impossible. The actual measurement was achieved by watching the target angles from a real person, who was asked to make the same posture at each specific time set. This implies that small observational errors could be involved due to the role play. In addition, since the angles  $q_5$  and  $q_6$  were measured with the terminal side from the wrist to the center of racket, it was different from the actual wrist rotation and may overpass to the anatomical limitation of the wrist structure.

## Conversion of Discrete Data

It was difficult to simulate the smooth motion with the discrete data we obtained. An alternative way to resolve this problem is through numerical interpolation theories. These numerical methods allow investigators to determine the continuous swing motion by replacing the discrete data with smooth functions. The most simple and popular interpolation method is polynomial fitting [21]. This method is beneficial in that the function produced is continuously differentiable because of the property of polynomials. Each discrete angle sequence over the time interval is approximated with a distinct polynomial of less than 18 degrees.

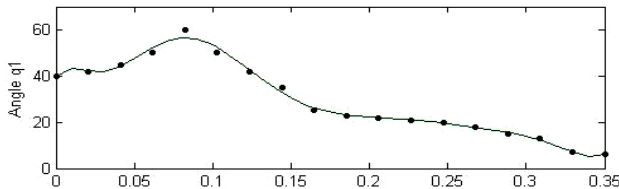


Figure 4. Polynomial interpolation of degree 10

Figure 4 shows how the polynomial fitting to angle  $q_1$  works with the polynomial of degree 10. As illustrated in Figure 4, the polynomial skips some nodes and does not work satisfactorily to cover the entire range of data. These mismatches occur even on the polynomials of higher degrees.

Instead, Figures 5 - 6 show the graphical simulations for the cubic spline interpolation for each angle parameter  $q_1$  through  $q_6$  in MATLAB. Even though this interpolation has only second differentiable properties, it was adequate to simulate a smooth motion.

## Simulation of the Swing Motion

Since Federer's arm size is not well-defined in the literature, lengths of the upper arm and the lower arm were selected at 28.04 cm and 30.69 cm, respectively, for  $l_1$  and  $l_2$  in

equations 4a-d. These values come from the data of Reeves's experimental subjects [22]. Taking normal sizes of upper and lower arms is also beneficial for general application to the public. The racket used for the simulation is the Topspin 660 Powerlite, manufactured since the late 1990s. The  $l_3$  value in the simulation, that is the length from the wrist point to the center of the racket, was  $53.20 + 3.00$  cm = 56.20 cm [23].

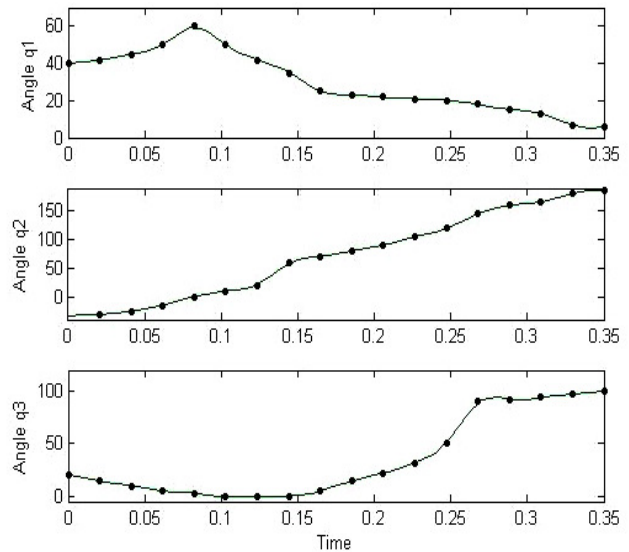


Figure 5. Cubic spline interpolation of  $q_1$  through  $q_3$

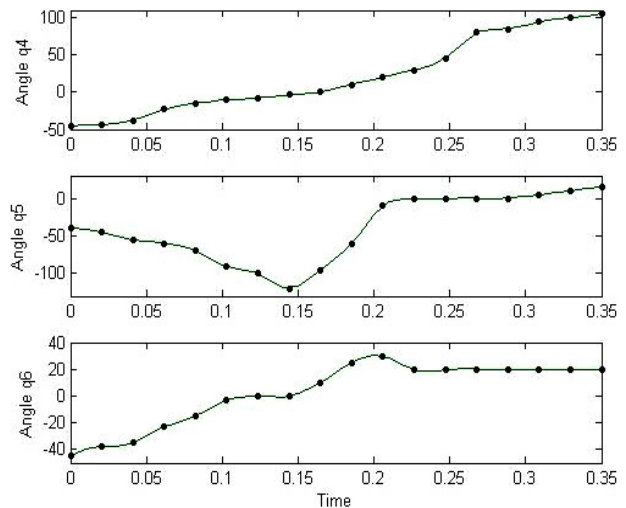
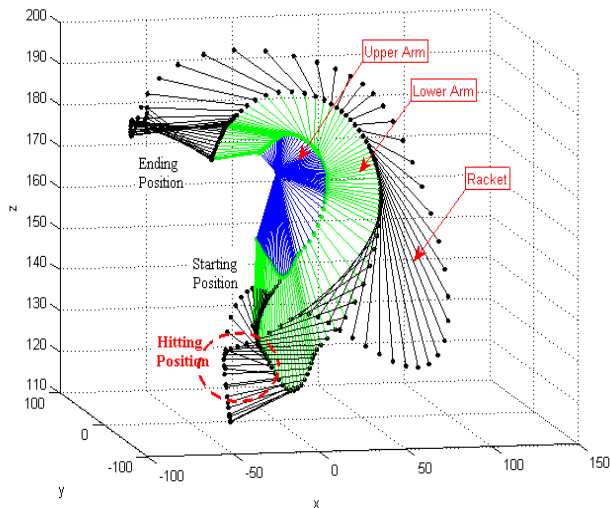


Figure 6. Cubic spline interpolation to  $q_4$  through  $q_6$

By observing the pictures of tennis players, the distance from the wrist point to the butt of the racket was determined to be 3.00 cm. Applying these values to equations 4a-d under the assumption that the player's shoulder is fixed at a height of 170 cm, Figure 7 shows how the player makes the full swing motion. Each group of three lines in Figure 7 is

marked at 0.0035-second intervals (100 marks/0.35 seconds). In the simulation, the dense plot explains the decrement of motion speed. The figure also shows that the player's swing proceeds along a very smooth trajectory and the player tries to make a fast and technically correct swing at the moment of impact.



**Figure 7.** Simulation of the full swing motion over the time interval 0.35 seconds (Unit: cm)

## Analysis of the Swing

A critical aspect of the forehand stroke is how fast the ball comes off the racket. The final shot speed is determined by the sum of bounce speed and racket speed:

$$\text{Shot speed} = \text{Bounce speed} + \text{Swing speed} \quad (6)$$

Bounce speed is mainly concerned with the tennis racket's unique parameters such as the local weight, the center of percussion, frame stiffness, and string-bed stiffness [24], [25]. Even if the racket's contribution to the final shot is factored out, the swing speed—the speed of the racket just prior to impact—is the most significant factor and has a huge influence on the ball's final outgoing speed. In Figure 8, the dotted curve in the upper graph shows this swing speed. From the graph, it can be seen that the ball collision occurs between roughly 0.15 and 0.2 seconds. One can also see that the player is able to increase ball speed by concentrating on the point of impact.

The other graph in Figure 8 shows the acceleration of each joint point. Since the acceleration values are directly proportional to the input/output force combining with the segmental mass, it works as a significant factor for determining how the player controls the force over a full swing. As shown in the lower graph in Figure 8, the greatest force is applied at

the point of impact. After a required sequential motion, the player intended to decrease the force from the body at around 0.27 seconds.

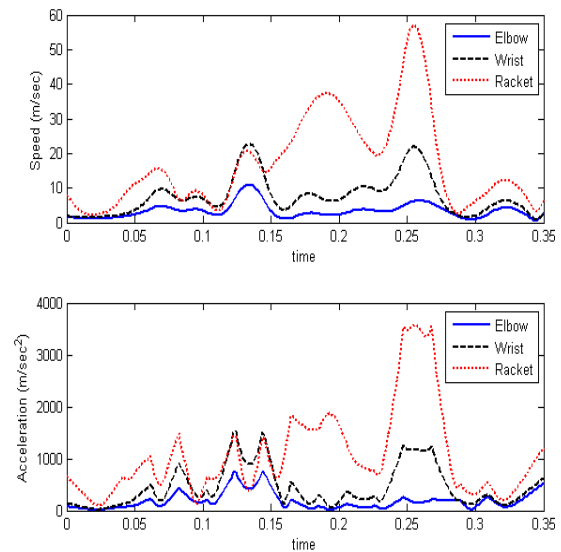


**Figure 8.** Speed (above) and acceleration (below) of the elbow point, the wrist point and the center of racket over the full swing

Humans act in such a way as to minimize certain types of cost functions or human performance measures such as reachability, dexterity, musculoskeletal discomfort, fatigue, torque, stress, etc. A number of studies noted a variety of methods for finding such optimized paths through the process of optimization of base-motion prediction [26]-[30]. However, having found motion paths through simulation, this study focused on the evaluation of the existing cost functions. In particular, the authors considered stress functions and potential-energy functions according to vertical-directional shifting.

The stress function concerns discomfort, due to the displacement of joint angles; this was mathematically defined as an aggregate weighted function by

$$f_{\text{stress}}(q) = \sum_{i=1}^{DOF} \omega_i |q_i - q_i^N| \quad (7)$$

where  $q_i^N$  represents the  $i^{\text{th}}$  joint angle in the neutral/equilibrium position, which may be different from the body models [27]-[29]. With the assumption of humans' tendency to gravitate to a comfortable neutral position, it was assumed that  $q_1^N = 90^\circ$  and  $q_2^N = q_3^N = q_4^N = q_5^N = q_6^N = 0$ . The set of weights,  $\omega_i$ , were mostly based on intuition and experimentation, assigning relative importance to the segmental components. In this study, the authors tested the three

types of weights: 1) segmental mass-based weights; 2) accumulated mass-based weights; and, 3) segmental length-based weights. Again considering the segmental masses, 2.17 kg, 1.27 kg, and 0.48+0.35 kg for the upper arm, lower arm, and the hand-to-racket link, respectively [22], [23], the segmental mass-based weights were given as the ratio  $\omega_1: \omega_2: \omega_3: \omega_4: \omega_5: \omega_6 = 2.17:2.17:1.27:1.27:0.83:0.83$ . Meanwhile, with the assumption that the upper-arm motion is restricted by the mass of both the lower arm and hand, and the lower-arm motion is limited by the mass of the hand, the accumulated mass-based weights are given as  $\omega_1: \omega_2: \omega_3: \omega_4: \omega_5: \omega_6 = 4.27:4.27:2.10:2.10:0.83:0.83$ .

Finally the length-based weights are taken as  $\omega_1: \omega_2: \omega_3: \omega_4: \omega_5: \omega_6 = 28.04:28.04:30.69:30.69:56.02:56.02$ . Figure 9 shows the calculation of stress factors due to the joint angles  $q_1$  through  $q_n$  (upper graph) and the total stress value according to the weighted types (lower graph). As shown in Figure 9, biomechanical stress continues to increase along the swing regardless of weighted types. It was accepted as reasonable that the ending posture of the swing looked very uncomfortable when compared to the normal relaxed posture.

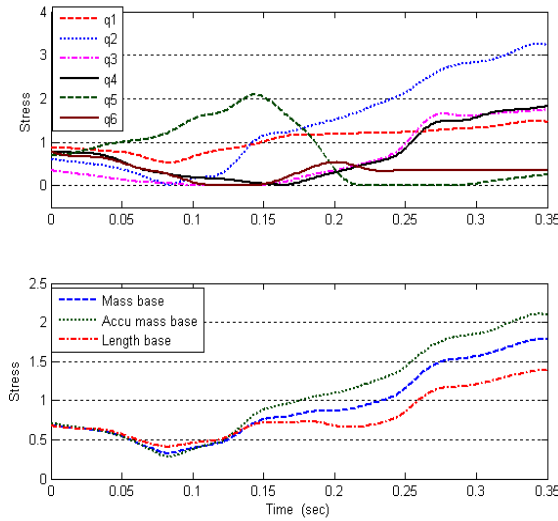


**Figure 9. Stress factors according to the joint angles (upper graph) and overall stress according to the different sets of weight (lower graph)**

The potential energy also works as a critical factor to constrain the human movement. It is mainly divided into two categories; potential energy stored in the muscles and potential energy due to gravity. This study focused on the latter, which was indirectly based on the vertical directional movement of each mass segment. Then, the total potential energy was calculated as a weighted sum of segmental potential energy as

$$f_{potential}(q) = \sum_{i=1}^{DOF} P_i = \sum_{i=1}^{DOF} (-m_i g h_i) \quad (8)$$

Here,  $h_i$  represents the height of each center of segmental mass [28]. However, if this potential energy function is used directly in order to minimize this factor, there would always be a tendency to bend over. Consequently, the change in potential energy from one of the initial configurations to one of the updated configurations was minimized. Such a potential energy is defined by

$$f_{\Delta potential}(q) = \sum_{i=1}^{DOF} P_i = \sum_{i=1}^{DOF} (-m_i g)^2 (\Delta h_i)^2 \quad (9)$$

[29], [30]. Figure 10 illustrates the total potential energy (upper graph) and the change of potential energy (lower graph) along the full swing motion. As observed in Figure 10, the total potential energy was almost re-tracing the graph of the z-coordinate of the simulation. Meanwhile, the lower graph in the figure reflects the fact that at the impact moment, a huge amount of energy conversion occurs for power hitting. The reason that the energy change stays at the lower level after the point of impact is understood because the player must correctly control the ball.

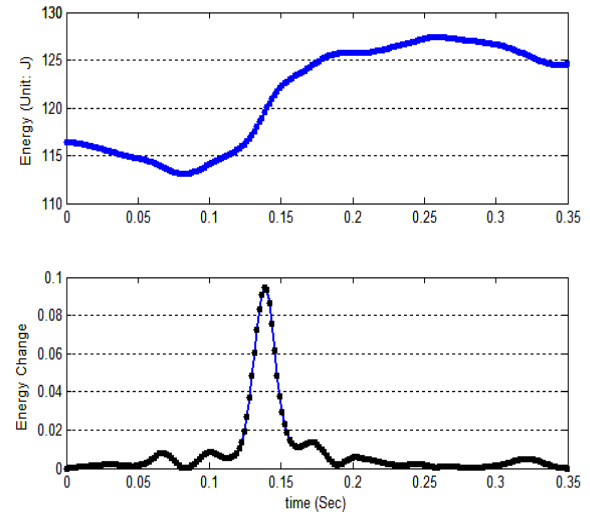


**Figure 10. Potential energy (upper graph) and the change in the potential energy (lower graph) along the full swing motion**

In addition to the constraint factors noted above, one can consider other constraint functions, which can be evaluated based on this simulation; for example,

$$f_{inconsistency}(q) = \sum_{i=1}^{DOF} \omega_i |q_i(t)| \quad (10a)$$

$$f_{\text{nonsmoothness}}(q) = \sum_{i=1}^{DOF} \omega_i (q_i(t))^2 \quad (10b)$$

[28], [29]. Although constraint functions were examined individually, in order to yield the maximum effect, such performance measures must be used in a combined manner. Obviously, a new weight for each function must also be developed according to the relative effectiveness of the motion restriction.

## Summary

Developing a model for the most effective technique was more difficult for open-skill sports. That is, the factors affecting the performance of the forehand stroke in tennis are numerous. Sometimes one may be confronted with combinations of factors, which the player is able or unable to control. These factors include player's location on the court, opponent's location on the court, the incoming direction and velocity of the ball, offensive or defensive situation, material status of the court and even weather. Even player's physical status and condition should be considered. Therefore, the best way to make the perfect forehand swings depends on how much the player practices against a certain situation.

This study described the overall procedures of how to computationally simulate the human movement through a tennis player's forehand swing and how to analyze the simulation biomechanically. Regardless of available equipment or lack of informed sources, the procedure of analysis of the player's motion is still valuable from the standpoint of the public's understanding of the subject.

There are many different issues concerning the human motion needing to be analyzed. Subsequent studies should include a direct extension of this modeling to more complex modeling, and a comparative analysis of these results to the optimization-based motion paths, so that a well-defined realistic human motion on the given tasks can be found.

## References

- [1] W. Kuehn, "Digital Factory - Simulation enhancing the product and production engineering process", proceeding of the 38<sup>th</sup> conference on winter simulation: Manufacturing applications: manufacturing systems design, pp 1899-1906, 2006
- [2] A. Fireman, and N. Lesinski, "Virtual Ergonomics: Taking human factors into account for improved product and process", 2009 Dassault Systemes Delmia Corp, 2009
- [3] K. Jung, O. Kwon, and H. You, "Development of a digital human model generation method for ergonomic design in virtual environment", *Inter. J. of Industrial Ergonomics*, Vol. 39(5), pp 744-748, 2009
- [4] S.A. Gill, and R.A. Ruddle, "Using virtual humans to solve real ergonomic design problems", *Simulation* 98. Inter. Conference. (Publ. No. 457), 1998
- [5] J. Yang, T. Sinokrot, K. Abdel-Malek, S. Beck, and K. Nebel, "Workspace zone differentiation and visualization for virtual humans", *Ergonomics*, Vol. 51(3), pp 395-413, 2008
- [6] P.A. Hancock, and R. Parasuraman, "Human factors and safety in the design of intelligent Vehicle-Highway Systems (IVHS)", *J. of Safety Research*, Vol. 23, pp. 181-198, 1992
- [7] N. Pelechano, and A. Malkawi, "Evacuation simulation models: Challenges in modeling high rise building evacuation with cellular automata approaches", *Automation in Construction*, Vol. 17(4), pp 377-385, 2008
- [8] D. Andrews, F. Moses, H. Hawkins, M. Dunaway, R. Matthews, and T. Singer, "Recent Human Factors Contributions to Improve Military Operations", *Human Factors and Ergonomics Society Bulletin*, Vol. 46(12), 2003
- [9] R.W. Pew, and A.S. Movor, "Modeling human and organizational behavior: application to military simulation", National Academic Press, 2001
- [10] X. Man, C. Swan, and S. Rahmatallah, "A Clothing Modeling Framework for Uniform and Armor System Design", *Proc. SPIE*, 2006
- [11] S.R. Carvalho, R. Boulic, and D. Thalmann, "Interactive low-dimensional human motion synthesis by combining motion model and PIK", *Comp. Anim. Virtual Worlds*, Published online in Wiley Inter-Science, 2007
- [12] S.M. Nesbit, and M. Serrano, "Work and power analysis in the golf swing", *J. of Sports Science and Medicine*, Vol. 4, pp 520-533, 2005
- [13] P. McGinnis, "Biomechanics of sports and exercise", *Human Kinetics*, 2005
- [14] G. Robertson et al, "Research Methods in Biomechanics", *Human Kinetics*, 2004
- [15] J. Dapena, "Simulation of modified human airborne movements", *J. of Biomechanics*, Vol. 14, pp 81-89, 1981
- [16] M.R. Yeadon, J. Atha, and F.D. Hales, "The simulation of aerial movement-IV: A computer simulation model", *Journal of Biomechanics*, Vol 23(1), pp 85-89, 1990
- [17] L. Sciavicco, and B. Siciliano, "Modeling and control of robot manipulators", McGraw-Hill, 1996
- [18] P. Allard, L. Stokes, and J.P. Blanchi, "Three-dimensional analysis of human movement", *Human kinetics*, 1995

- 
- [1] J. Denavit, and R.S. Hartenberg, "A kinematic notion for lower-pair mechanisms based on matrices", Journal of Applied Mechanics, Vol. 77, pp 215-221, 1955
- [2] K. Atkinson, and W. Han, "Elementary Numerical Analysis", Wiley & Sons, Inc, 2004
- [3] URL [www.tennis-warehouse.com/player.html?ccode=rfederer](http://www.tennis-warehouse.com/player.html?ccode=rfederer) (Last accessed on April 1, 2010)
- [4] R.A. Reeves, O.D. Hicks, and J.W. Havalta, "The relationship between upper arm anthropometrical measures and vertical jump displacement", Int. J. of Exercise Science, Vol. 2(4), 2008
- [5] R. Cross, "Customising a tennis racket by adding weights", Sport Engineering, Vol. 4, pp 1-14, 2001
- [6] URL [http://twu.tennis-warehouse.com/learning\\_center/racquetcontribution.php](http://twu.tennis-warehouse.com/learning_center/racquetcontribution.php) (Last accessed on April 1, 2010)
- [7] H. Brody, "Physics of the tennis racket", American J. of Physics, Vol. 47(6), pp 482-487, 1979
- [8] I. Rodriguez, R. Boulic, and D. Meziat, "A joint – level model of fatigue for the postural control of virtual humans", J. of Three Dimensional Images, Vol. 17(1), pp 70–75, 2003
- [9] T. Marler, S. Rahmatalla, M. Shanahan, and K. Abdel-Malek, "A new discomfort function for optimization-base posture prediction", [2005 Digital Human Modeling for Design and Engineering Symposium, June 2005](#) or SAC international, DN 2005-01-2680, 2005
- [10] URL <http://www.santoshumaninc.com/pdf/vsr-motion.pdf> (last accessed on April 1, 2010)
- [11] J. Yang, T. Marler, H. Kim, J. Arora, and K. Abdel-Malek, "Multi-objective optimization for upper body posture prediction", Proc. 10th AIAA/ISSMO Multidisciplinary Analysis and Optimization Conf, 2004
- [12] E.N. Horn, "Optimization-based dynamic human motion prediction", master degree thesis, U. of Iowa, 2005

zation-based renewable energy systems. Dr. Oh may be reached at [hoh@savannahstate.edu](mailto:hoh@savannahstate.edu)

**ONAJE LEWIS** is currently a junior in Mechanical Engineering program at Georgia Institute of Technology at Savannah. His interests are in the mechanical design of vehicle body. Mr. Lewis may be reached at [onaje\\_lewis@hotmail.com](mailto:onaje_lewis@hotmail.com)

**ASAD YOUSUF** is Professor of Electronics Engineering Technology at Savannah State University. He earned his B.S. (Electrical Engineering, 1980) from N.E.D University, MS (Electrical Engineering, 1982) from the University of Cincinnati, and a Doctoral degree (Occupational Studies, 1999) from the University of Georgia. Dr. Yousuf is a registered professional engineer in the state of Georgia. He is also a Microsoft Certified Systems Engineer (MCSE). Dr. Yousuf has worked as a summer fellow at NASA, US Air Force, US Navy, Universal Energy Systems, Oakridge National Laboratory, and Lockheed Martin. Dr. Yousuf may be reached at [yousufa@savannahstate.edu](mailto:yousufa@savannahstate.edu)

**SUJIN KIM** has been serving as an Assistant Professor of Mathematics at Savannah State University. Her research interest involves wavelet theory in statistics and digital image processing through wavelet. Dr. Kim may be reached at [kims@savannahstate.edu](mailto:kims@savannahstate.edu)

## Biographies

**HYOUNKYUN OH** is an Assistant Professor of Mathematics at Savannah State University. He instructs undergraduate mathematics courses, directs undergraduate research, and performs research involved with computational differential algebraic equations, human-factor based biomechanics, application of digital image processing, and optimi-